Second-order resummed thermodynamic perturbation theory for central-force associating potential: Multi-patch colloidal models

Y. V. Kalyuzhnyi,[1,a)] B. D. Marshall,[2] W. G. Chapman,[2] and P. T. Cummings[3]
[1]*Institute for Condensed Matter Physics, Svientsitskoho 1, 79011 Lviv, Ukraine*
[2]*Department of Chemical and Biomolecular Engineering, Rice University, 6100 S. Main, Houston, Texas 77005, USA*
[3]*Department of Chemical Engineering, Vanderbilt University, Nashville, Tennessee 37235-1604, USA and Center for Nanophase Material Sciences, Oak Ridge National Laboratory, Oak Ridge, Tennessee 37831-6494, USA*

(Received 11 April 2013; accepted 7 July 2013; published online 26 July 2013)

We propose a second-order version of the resummed thermodynamic perturbation theory for patchy colloidal models with arbitrary number of multiply bondable patches. The model is represented by the hard-sphere fluid system with several attractive patches on the surface and resummation is carried out to account for blocking effects, i.e., when the bonding of a particle restricts (blocks) its ability to bond with other particles. The theory represents an extension of the earlier proposed first order resummed thermodynamic perturbation theory for central force associating potential and takes into account formation of the rings of the particles. In the limiting case of singly bondable patches (total blockage), the theory reduces to Wertheim thermodynamic perturbation theory for associating fluids. Closed-form expressions for the Helmholtz free energy, pressure, internal energy, and chemical potential of the model with an arbitrary number of equivalent doubly bondable patches are derived. Predictions of the theory for the model with two patches appears to be in a very good agreement with predictions of new NVT and NPT Monte Carlo simulations, including the region of strong association. © *2013 AIP Publishing LLC*. [http://dx.doi.org/10.1063/1.4816128]

I. INTRODUCTION

In this paper we continue our study of patchy colloidal models with an arbitrary number of multiply bondable patches. In the previous two papers[1,2] thermodynamic perturbation theory for central force (TPT-CF) associating potential,[3–5] which was formulated for one multiply bondable attractive site, placed in the center of the particle, was extended to account for blocking effects, i.e., when the bonding of a particle restricts (blocks) its ability to bond with other particles. The theory, which we call resummed TPT-CF (RTPT-CF) was applied to describe the properties of multiply bondable one-patch[1] and multi-patch[2] models of associating fluid. Subsequently, Wertheim's two-density TPT for the one-patch model[6] was extended to account for the possibility of multiple bonding.[7,8] This goal was achieved by taking into account three-particle correlations and allowing for chain and three-particle ring formation. Here we formulate the second-order version of the RTPT-CF theory (RTPT2-CF) for the models with arbitrary number of multiply bondable patches. Ring formation is taken into account by inclusion of three body correlations as discussed in Refs. 7 and 8. These rings consist of three doubly bonded patches which are different, with a different ring graph, than those previously considered.[9]

Patchy colloids are colloidal particles with the surface patterned such that there are attractive patches. The interactions of these colloids can be controlled by varying the number, size, and interaction strength of these patches.[10–12] Most often theoretical studies of such colloidal particles are carried out using the models of the type developed by Bol[13] and extended further by Nezbeda and co-workers,[14–16] Jackson *et al.*,[17] and Kern and Frenkel.[18] Typically, the model is represented by hard spheres with an orientationally dependent attractive interaction mediated by off-center square-well or anisotropic square-well sites with angular cutoff (conical sites). In the last few decades a substantial amount of work has been carried out on the theoretical description of the structural and thermodynamic properties of these types of models[17,19–33] (see also the review papers of Sciortino,[34] Bianchi *et al.*[35] and references therein). However, since all these studies are based on the theory for associating fluids developed by Wertheim,[6,36,37] they are focused on the versions of the models with singly bondable sites only.

In this study we propose a second-order version of the thermodynamic perturbation theory[2] for multiple patch colloids with doubly bondable patches. In the limiting case of the patch coverage allowing only one bond per site our theory reduces to TPT of Wertheim.[36,37] To validate the accuracy of the approximations made we compare theoretical predictions for the two-patch model against computer simulation predictions. In these simulations we allow maximum patch coverages which can accommodate up to four bonds per patch.

The paper is organized as follows: in Sec. II we present the potential model and in Sec. III we derive RTPT2-CF theory for multipatch hard-sphere fluid and present the final expressions for thermodynamics of the model with n_s equivalent doubly bondable patches. In Sec. IV we discuss details of the

a)Author to whom correspondence should be addressed. Electronic mail: yukal@icmp.lviv.ua

computer simulations and compare theoretical and simulation predictions for the two-patch version of the model. Finally, our conclusions are collected in Sec. V.

II. THE MODEL

We consider a one-component hard-sphere fluid with a number density ρ at a temperature T ($\beta = 1/k_BT$). In addition to the hard-sphere interaction Φ_{hs} the particles are interacting via a short-ranged square-well orientationally dependent associative potential Φ_{ass} of the type proposed by Bol,[13] Jackson *et al.*[17] and Kern and Frenkel.[18] The corresponding total pair potential Φ is given by

$$\Phi(12) = \Phi_{hs}(r) + \Phi_{ass}(12), \tag{1}$$

where 1 and 2 denote positions and orientations of the particles 1 and 2. We assume that the associative part of the potential can be represented as a sum of n_s^2 site-site terms Φ_{KL}, i.e.,

$$\Phi_{ass}(12) = \sum_{KL}^{n_s} \Phi_{KL}(12), \tag{2}$$

where

$$\Phi_{KL}(12) = \begin{cases} -\epsilon_{KL}, & \text{for} \quad d \le r \le r_{KL}^{(c)}, \quad \theta_{K1} \le \theta_K^{(c)} \quad \text{and} \quad \theta_{L2} \le \theta_L^{(c)} \\ 0, & \text{otherwise} \end{cases}. \tag{3}$$

Here d is the hard-sphere diameter, the lower indices K and L denote conical square-well sites and take n_s values A, B, C, ... The term θ_{K1} (θ_{L2}) is the angle between the line connecting the centers of the two particles 1 and 2, and the line connecting the center of the particle 1 (2) and its site K (L), ϵ_{KL} and $r_{KL}^{(c)}$ are defined to be the square-well depth and width, respectively, and r is the distance between the centers of the two particles. In the limiting case of sticky interaction i.e., for $r_{KL}^{(c)} - d \to 0$ (and $\epsilon_{KL} \to \infty$), and for $0 \le \theta_K^{(c)} < 30^\circ$ attractive site K can be bonded only once. For $30^\circ \le \theta_K^{(c)} < 35.3^\circ$ the maximum number of bonds per site is two, for $35.3^\circ \le \theta_K^{(c)} < 45^\circ$ this number is three and for $45^\circ \le \theta_K^{(c)} < 58.3^\circ$ the site K can bond simultaneously four particles. In the present study we will be using finite value for the potential well width (and depth) assuming, that the above sequence of the limiting bonding angles will be unchanged. For sufficiently narrow potential well this assumption is expected to be accurate. Hereafter, we will assume also that the maximum number of bonds per site is two.

In what follows we will be using the Mayer functions for the hard-sphere interaction f_{hs} and for the site-site associative interaction f_{KL}, i.e.,

$$f_{hs}(r) = \exp\{-\beta\Phi_{hs}(r)\} - 1 \quad \text{and}$$
$$f_{KL}(12) = \exp\{-\beta\Phi_{KL}(12)\} - 1. \tag{4}$$

III. THEORY

A. Notation and basic relationships

In this subsection we briefly discuss the notation used and basic relationships. To avoid unnecessary repetition we refer the readers to the original papers for more details.[2,36,37] According to the diagrammatic analysis, carried out in Refs. 1–5, the Helmholtz free energy A of the model at hand in excess to its hard-sphere reference system value A_{hs}, i.e., $\Delta A = A - A_{hs}$, can be written in the following form:

$$\beta\Delta A = \int \left[\rho(1) \ln \frac{\sigma_{\{0\}}(1)}{\rho(1)} - \rho(1) + \sum_{\{i\}\neq\{0\}}^{\{2\}} \sigma_{\{i\}}^*(1) c_{\{i\}}(1) \right] \times d(1) - \Delta c^{(0)}, \tag{5}$$

where $d(1)$ denotes integration over position and orientation of the particle 1: for uniform systems all quantities under the integral become constant. Here the lower indices $\{i\}$ specifies the bonding state of the corresponding particles, i.e.,

$$\{i\} \equiv i_A, i_B, i_C, \ldots, \tag{6}$$

where i_K take the values 0, 1, 2 and denote nonbonded, singly or doubly bonded states of the site K, respectively. In what follows in the special case, when in the set $\{i\}$ all indices, except one index i_K, are equal 0 the corresponding bonding state of the particle will be denoted as K_{i_K}, i.e., $\{i\} = 0, 0, \ldots, i_K, \ldots, 0, 0 \equiv K_{i_K}$.

In (5) the density parameters $\sigma_{\{i\}}$ are connected to the density of the particles $\rho_{\{j\}}$ via the following relation

$$\sigma_{\{i\}}(1) = \sum_{\{j\}=\{0\}}^{\{i\}} \rho_{\{j\}}(1) \equiv \sum_{j_A, j_B, j_C, \ldots = 0}^{i_A, i_B, i_C, \ldots} \rho_{j_A, j_B, j_C, \ldots}(1), \tag{7}$$

and $\Delta c^{(0)} = c^{(0)} - c_{hs}^{(0)}$ is the contribution to the fundamental graph sum due to association. For the purpose of diagrammatic analysis we follow Wertheim[36] and instead of circles we introduce hypercircles to represent particles in diagrammatic expansions. Each hypercircle is depicted as a large open circle with small circles inside denoting the sites. Corresponding cluster integrals are represented by the diagrams build on hypercircles connected by f_{hs} and $e_{hs} = f_{hs} + 1$ bonds and site circles connected by the associating bonds f_{KL}. We allow a maximum of two associating bonds per site. Double

bonding between the pair of hypercircles is not allowed. Each hypercircle in a bonding state $\{i\}$ contains as a factor of the density parameter $\sigma^*_{\{i\}} \equiv \sigma_{\{2-i\}}$, where $\{2-i\} \equiv 2-i_A$, $2-i_B, 2-i_C, \ldots$. We have

$c^{(0)}$ = sum of all topologically distinct irreducible diagrams consisting of s-mer diagrams with $s = 1, \ldots, \infty$ and f_{hs} bonds between pairs of hypercircles in distinct s-mer diagrams. All hypercircles are field circles carrying the σ-factor according to the rule formulated above.

Here s-mer diagrams are the diagrams consisting of s hypercircles, which are all connected by the network of f_{KL} bonds, e_{hs} bonds between pairs of hypercircles connected directly by f_{KL} bond and f_{hs} bonds placed in all possible ways between pairs of hypercircles not connected directly by e_{hs} bond. $c^{(0)}_{hs}$ is the sum of all diagrams entering $c^{(0)}$, which are devoid of associating bonds f_{KL}.

Functional differentiation of $c^{(0)}$ with respect to $\sigma^*_{\{i\}} \equiv \sigma_{\{2-i\}}$ gives an expression for $c_{\{i\}}$:

$$c_{\{i\}}(1) = \frac{\delta c^{(0)}}{\delta \sigma^*_{\{i\}}(1)}. \tag{8}$$

B. RTPT2-CF theory for multi-patch hard-sphere fluid

To proceed one has to approximate the fundamental graph sum $\Delta c^{(0)}$. In the current model we allow a maximum of two bonds per site. For this case $\Delta c^{(0)}$ must contain contributions for single and double bonded sites.[1,2,7] We employ the single chain approximation which states that we only consider diagrams with a single path of attraction bonds connecting patches. The double bonded sites can exist in chains or triatomic rings of doubly bonded sites. We account for these rings by inclusion of a three point ring diagram consisting of three particles each with one double bonded site.[7] According to these approximations, which will be specified below, the only density parameters, which appear in $\Delta c^{(0)}$ are $\sigma^*_{K_1}$ and $\sigma^*_{K_2}$. Therefore, taking into account (8), we have

$$c_{\{i\}}(1) = 0, \tag{9}$$

where $\{i\} \neq \{0\}$, $\{i\} \neq 0, \ldots, 0, 1, 0, \ldots, 0$ and $\{i\} \neq 0, \ldots, 0, 2, 0, \ldots, 0$. Expressions for c_{K_1} and c_{K_2} can be obtained using relation between $\sigma_{\{i\}}$ and $c_{\{i\}}$, derived in Refs. 1 and 2. We obtain[2]

$$c_{K_1}(1) = \frac{\partial c^{(0)}}{\partial \sigma^*_{K_1}(1)} = \frac{\sigma_{K_1}(1)}{\sigma_{\{0\}}(1)} - 1 \tag{10}$$

and

$$c_{K_2}(1) = \frac{\partial c^{(0)}}{\partial \sigma^*_{K_2}(1)} = \frac{\sigma_{K_2}(1)}{\sigma_{\{0\}}(1)} - \frac{1}{2}\frac{\sigma^2_{K_1}(1)}{\sigma^2_{\{0\}}(1)} - \frac{1}{2}. \tag{11}$$

Combining the same relation between $\sigma_{\{i\}}$ and $c_{\{i\}}$ and equality (9) we obtain the following useful relation between the density parameters $\sigma_{\{i\}}(1)$:

$$\sigma^{n_s}_{\{0\}}(1)\sigma_{i_A,i_B,\ldots}(1) = \sigma_{\{0\}}(1)\sigma_{i_A}(1)\sigma_{i_B}(1)\ldots. \tag{12}$$

This relation was also derived in Ref. 2. Taking into account (12) and substituting $c_{\{i\}}$ in (5) by the corresponding expressions (9)–(11) gives

$$\beta\Delta A = \int \left\{\rho(1)\ln\frac{\sigma_{\{0\}}(1)}{\rho(1)} + \sum_K \left[\rho(1) - \sigma^*_{K_1}(1) + \frac{1}{2}\frac{\sigma^*_{K_2}(1)\sigma^2_{K_1}(1)}{\sigma^2_{\{0\}}(1)} - \frac{1}{2}\sigma^*_{K_2}(1)\right]\right\} \times d(1) - \Delta c^{(0)}. \tag{13}$$

Expression for the pressure P follows from the standard relation

$$PV = G - A = \int \rho(1)\frac{\partial A}{\partial \rho(1)}\, d(1) - A, \tag{14}$$

where G is the Gibbs free energy. We have

$$\beta\Delta PV = -\sum_K \left[\rho(1) - \sigma^*_{K_1}(1) + \frac{1}{2}\frac{\sigma^*_{K_2}(1)\sigma^2_{K_1}(1)}{\sigma^2_{\{0\}}(1)} - \frac{1}{2}\sigma^*_{K_2}(1)\right] d(1) + \Delta c^{(0)} - \int \rho(1)\frac{\partial \Delta c^{(0)}}{\partial \rho(1)}\, d(1). \tag{15}$$

The infinite sum of the diagrams, which is represented here by $\Delta c^{(0)}$, will be calculated combining chain and ring approximations,[1,2,7,37] i.e.,

$$\frac{\Delta c^{(0)}}{V} = \frac{1}{2}\sum_{KP}\bar\sigma^*_{K_1}\bar\sigma^*_{P_1}\sum_{n=0}^{\infty}\sum_{\underbrace{LM\ldots N}_{n}}\bar\sigma^*_{L_2}\bar\sigma^*_{M_2}\ldots\bar\sigma^*_{N_2}I^{(n+1)}_{KLM\ldots NP} + \frac{1}{6}\sum_{KLM}\bar\sigma^*_{K_2}\bar\sigma^*_{L_2}\bar\sigma^*_{M_2}R^{(2)}_{KLM}, \tag{16}$$

where

$$R^{(2)}_{KLM} = \Omega^{-2}\int d(2)d(3)f_{KL}(12)f_{LM}(23)f_{MK}(31)g_{hs}(123), \tag{17}$$

$$\underbrace{I^{(n)}_{KLM\ldots NP}}_{n+1} = \Omega^{-n}\int d(2)\ldots d(n+1)\; f_{KL}(12)f_{LM}(23)\ldots f_{NP}(n,n+1)G_{hs}(1\ldots n+1) \tag{18}$$

$\bar\sigma_{K_i} = \sigma_{K_i}(1)\Omega$, $\Omega = 8\pi^2$, $G_{hs}(1\ldots n)$ denotes the subset of diagrams from the set representing the n-particle hard-sphere monomer distribution function, which together with the chain of associative bonds $f_{KL}(12)\ldots f_{NP}(n-1, n)$ form an irreducible diagram.[37] This subset is approximated here by the corresponding subset representing the n-particle hard-sphere distribution function $g_{hs}(1\ldots n)$ and includes in addition to $g_{hs}(1\ldots n)$ itself products of s-particle hard-sphere distribution functions ($s < n$) obtained by all possible partitioning of the sequence of points $1, 2, \ldots, n$ into subsequences with a

common switching point, which carry the factor −1. For example, for $n = 2$, 3, and 4 we have[37]

$$\begin{aligned} G_{hs}(12) &= g_{hs}(12), \\ G_{hs}(123) &= g_{hs}(123) - g_{hs}(12)g_{hs}(23), \\ G_{hs}(1234) &= g_{hs}(1234) - g_{hs}(12)g_{hs}(234) \\ &\quad - g_{hs}(123)g_{hs}(34) \\ &\quad + g_{hs}(12)g_{hs}(23)g_{hs}(34). \end{aligned} \tag{19}$$

Following Wertheim[37] we express $G-$functions in terms of $E-$functions, which are obtained using the above representation for $G_{hs}(1\ldots n)$ with additional bond $e_{hs}(i-1, i+1)$ inserted between left and right nearest neighbor of each switching point i. According to this representation $G_{hs}(1\ldots n)$ includes $E(1\ldots n)$ and products of the lower-order E-functions, obtained by all possible partitioning of the sequence of the points 1, 2, …, n into subsequences with a common switching points i, each bypassed by the bond $f_{hs}(i-1, i+1)$. Now for $n = 2$, 3, and 4 we have[37]

$$\begin{aligned} G_{hs}(12) &= E(12), \\ G_{hs}(123) &= E(123) + E(12)f_{hs}(13)E(23), \\ G_{hs}(1234) &= E(1234) + E(12)f_{hs}(13)E(234) \\ &\quad + E(123)f_{hs}(24)E(34) \\ &\quad + E(12)f_{hs}(13)E(23)f_{hs}(24)E(34). \end{aligned} \tag{20}$$

Upon substitution of the above representation for G_{hs} in (18) the integral $I^{(n)}_{K\ldots P}$ will be expressed as a sum of the integrals over the products of the E-functions, supplemented by the chain of attractive bonds f_{KL}. Each of the terms in a sum has certain number of the switching points and summation is carried out over their number and position in the chain. Following Wertheim[37] we refer to the part of the chain diagram located between two consecutive switching points as a segment and denote the integral over m segments with $m-1$ switching points $s, t, \ldots, q$, which are associated with $m-1$ sites $S, T, \ldots, Q$ by $E^{(n,m)}_{K\ldots P}$,

$$\begin{aligned} E^{(n,m)}_{KLM\ldots NP} = \Omega^{-n} \int & d(2)\ldots d(n+1)\ f_{KL}(12)f_{LM}(23) \\ & \ldots f_{NP}(n, n+1) \\ & \times E(1\ldots s)f_{hs}(s_-, s_+)E(s\ldots t)f_{hs}(t_-, t_+) \\ & \ldots f_{hs}(q_-, q_+)E(q\ldots n+1), \end{aligned} \tag{21}$$

where $s_- = s-1$ and $s_+ = s+1$.

For the model with $\theta^{(c)}_K = 180^\circ$ or $\theta^{(c)}_K < 30^\circ$ and with sufficiently narrow width of the square-well (sticky) interaction this integral can be approximated by a corresponding product of the integrals over a single segments times the product of the factors L_K, i.e.,

$$\begin{aligned} E^{(n,m)}_{KLM\ldots NP} = (-1)^{m-1} & E^{(s-1,1)}_{K\ldots S}E^{(t-s,1)}_{S\ldots T} \\ & \ldots E^{(n-q,1)}_{Q\ldots P}L_S L_T \ldots L_Q, \end{aligned} \tag{22}$$

where

$$L_H = \frac{E^{(n,m)}_{K\ldots H\ldots P}}{E^{(n-h,m-j)}_{K\ldots H}E^{(h,j)}_{H\ldots P}} = \frac{E^{(2,2)}_{KHP}}{E^{(1,1)}_{KH}E^{(1,1)}_{HP}}, \tag{23}$$

and h and H denote the switching point and corresponding site, respectively. Note, that for the model with $\theta^{(c)}_K < 30^\circ$ all terms in (18), which include n-particle distribution functions with $n \geq 3$ are equal to zero and $L_H = E^{(2,2)}_{KHP}/(E^{(1,1)}_{KH}E^{(1,1)}_{HP}) = 1$.[1,2] For $\theta^{(c)}_K < 30^\circ$ each attractive site can be bonded only once and with $L_H = 1$ our theory reduces to the first order TPT of Wertheim.[1,2,37] Similar to our previous studies[1,2] we assume that relation (22) is also valid for the intermediate values of $\theta^{(c)}_K$, i.e., for $30^\circ \leq \theta^{(c)}_K \leq 180^\circ$. Now the series in (16) can be summed to yield the following expression for $\Delta c^{(0)}$:

$$\frac{\Delta c^{(0)}}{V} = \frac{1}{2}\sum_{LM}\bar{\sigma}^*_{L_1}\bar{\sigma}^*_{M_1}[\mathbf{D}^{-1}\mathbf{E}]_{LM} + \frac{1}{6}\sum_{KLM}\bar{\sigma}^*_{K_2}\bar{\sigma}^*_{L_2}\bar{\sigma}^*_{M_2}R^{(2)}_{KLM}, \tag{24}$$

where $\mathbf{D} = \mathbf{1} + \mathbf{E}\bar{\boldsymbol{\sigma}}^*_2\mathbf{L}$ and $\mathbf{L}$, $\bar{\boldsymbol{\sigma}}^*_2$ and $\mathbf{E}$ are the matrices with the elements $[\mathbf{L}]_{LM} = \delta_{LM}L_M$, $[\bar{\boldsymbol{\sigma}}^*_2]_{LM} = \delta_{LM}\bar{\sigma}^*_{M_2}$ and

$$\begin{aligned} [\mathbf{E}]_{LM} = E_{LM} = E^{(1,1)}_{LM} &+ \sum_K \bar{\sigma}^*_{K_2}E^{(2,1)}_{LKM} \\ &+ \sum_{KP}\bar{\sigma}^*_{K_2}\bar{\sigma}^*_{P_2}E^{(3,1)}_{LKPM} + \ldots. \end{aligned} \tag{25}$$

According to (24) $\Delta c^{(0)}$ can be written in the following form

$$\begin{aligned} \Delta c^{(0)} = \frac{1}{2}\sum_K \int \bar{\sigma}^*_{K_1}(1)\frac{\partial \Delta c^{(0)}}{\partial \bar{\sigma}^*_{K_1}(1)}\, d(1) \\ + \frac{1}{6}V\sum_{KLM}\bar{\sigma}^*_{K_2}\bar{\sigma}^*_{L_2}\bar{\sigma}^*_{M_2}R^{(2)}_{KLM}, \end{aligned} \tag{26}$$

which together with (10), (13), and (15) gives the following expressions for Helmholtz free energy and pressure:

$$\begin{aligned} \beta\Delta A = \int \Bigg\{ & \rho(1)\ln\frac{\sigma_{\{0\}}(1)}{\rho(1)} \\ & + \sum_K\left[\rho(1) - \frac{1}{2}\sigma^*_{K_1}(1) - \frac{1}{2}\sigma^*_{K_2}(1)\right]\Bigg\} d(1) \\ & - \frac{1}{6}V\sum_{KLM}\bar{\sigma}^*_{K_2}\bar{\sigma}^*_{L_2}\bar{\sigma}^*_{M_2}R^{(2)}_{KLM} \end{aligned} \tag{27}$$

and

$$\begin{aligned} \beta\Delta PV = & -\sum_K\int\left[\rho(1) - \frac{1}{2}\sigma^*_{K_1}(1) - \frac{1}{2}\sigma^*_{K_2}(1)\right]d(1) \\ & + \frac{1}{6}V\sum_{KLM}\bar{\sigma}^*_{K_2}\bar{\sigma}^*_{L_2}\bar{\sigma}^*_{M_2}R^{(2)}_{KLM} \\ & - \int\rho(1)\frac{\partial\Delta c^{(0)}}{\partial\rho(1)}d(1). \end{aligned} \tag{28}$$

The density parameters $\sigma_{\{0\}}$, $\sigma^*_{K_1}$, and $\sigma^*_{K_2}$, which enter these expressions, follow from the solution of the set of equations formed by (10)–(12), i.e.,

$$\sum_L \bar{\sigma}^*_{L_1}[\mathbf{D}^{-1}\mathbf{E}]_{LA} = \frac{\bar{\sigma}_{A_1}(1)}{\bar{\sigma}_{\{0\}}(1)} - 1 \tag{29}$$

$$\frac{1}{2}\sum_{LM}\left\{\bar{\sigma}^*_{L_1}\bar{\sigma}^*_{M_1}\left[\mathbf{D}^{-1}\frac{\partial \mathbf{E}}{\partial \bar{\sigma}^*_{A_2}} - \mathbf{D}^{-1}\left(\frac{\partial \mathbf{E}}{\partial \bar{\sigma}^*_{A_2}}\bar{\boldsymbol{\sigma}}^*_2\mathbf{L} + \mathbf{E}\boldsymbol{\Delta}_A L_A\right)\mathbf{D}^{-1}\mathbf{E}\right]_{LM} + \bar{\sigma}^*_{L_2}\bar{\sigma}^*_{M_2}R_{LMA}\right\} = \frac{\sigma_{A_2}(1)}{\sigma_{\{0\}}(1)} - \frac{1}{2}\frac{\sigma^2_{A_1}(1)}{\sigma^2_{\{0\}}(1)} - \frac{1}{2}, \tag{30}$$

$$\bar{\sigma}_{A_1}\bar{\rho} = \bar{\sigma}^*_{A_1}\bar{\sigma}_{A_2}, \quad \bar{\sigma}_{\{0\}}\bar{\sigma}^*_{A_1} = \bar{\sigma}^*_{A_2}\bar{\sigma}_{A_1}, \quad \bar{\sigma}^{n_s-1}_{\{0\}}\bar{\rho} = \prod_{K=A}\bar{\sigma}_{K_2}, \tag{31}$$

where $[\boldsymbol{\Delta}_A]_{LM} = \delta_{LA}\delta_{MA}$.

Thus thermodynamical properties of the model at hand can be calculated, provided that expression for the infinite sum of diagrams E_{LM} (25) is available. Because our knowledge of the hard-sphere n-particle distribution functions for $n \geq 4$ is scarce we will approximate this series terminating it on the second term, i.e., assuming that for $n \geq 4$ $E^{(n,1)}_{L\ldots P} = 0$.

C. RTPT2-CF theory for the model with n_s equivalent patches

In this subsection we will formulate RTPT2-CF for the version of the model with n_s equivalent attractive sites. Taking into account this feature of the model expressions (24), (27), and (28), and relations (29)–(31) can be substantially simplified. For $\Delta c^{(0)}$ we have

$$\frac{\Delta c^{(0)}}{V} = \frac{1}{2}n_s^2\left(\frac{\bar{\sigma}^{*2}_1 E}{D} + \frac{1}{3}n_s\bar{\sigma}^{*3}_2 R^{(2)}\right), \tag{32}$$

where $E = E^{(1,1)} + n_s\bar{\sigma}^*_2 E^{(2,1)}$, $D = 1 + n_s L\bar{\sigma}^*_2 E$ and we have used condensed notation omitting the indices, which denote the type of the patches, i.e., for any quantity $x_{K_{i_K}}$ or X_K we have

$$x_{K_1} = x_{L_1} \equiv x_1, \quad x_{K_2} = x_{L_2} \equiv x_2, \quad X_K = X_L \equiv X. \tag{33}$$

Now self-consistent relations between the density parameters (29)–(31) will take the following form:

$$\frac{n_s\bar{\sigma}^*_1 E}{D} = \frac{\bar{\sigma}_1}{\bar{\sigma}_0} - 1, \tag{34}$$

$$\frac{1}{2}n_s^2\left[\frac{\bar{\sigma}^{*2}_1}{D^2}\left(E^{(2,1)} - LE^2\right) + \bar{\sigma}^{*2}_2 R^{(2)}\right] = \frac{\bar{\sigma}_2}{\bar{\sigma}_0} - \frac{1}{2}\frac{\bar{\sigma}^2_1}{\bar{\sigma}^2_0} - \frac{1}{2}, \tag{35}$$

and

$$\bar{\sigma}_1\bar{\rho} = \bar{\sigma}^*_1\bar{\sigma}_2, \quad \bar{\sigma}_0\bar{\sigma}^*_1 = \bar{\sigma}^*_2\bar{\sigma}_1, \quad \bar{\sigma}^{n_s-1}_0\bar{\rho} = \bar{\sigma}^{n_s}_2. \tag{36}$$

The solution of this set of equations reduces to the solution of the seventh order polynomial equation for $\gamma = \bar{\sigma}_0/\bar{\sigma}_2$, i.e.,

$$\sum_{i=0}^{7} a_i\gamma^i = 0, \tag{37}$$

where expressions for the polynomial coefficients a_i are presented in the Appendix A. The Helmholtz free energy (27) and pressure (28) can now be given in terms of the γ-parameter, i.e.,

$$\frac{\beta\Delta A}{N} = n_s\left\{\ln\gamma + \left[1 - \frac{1}{2}(\tau+1)\gamma\right] - \frac{1}{6}n_s^2\bar{\rho}^2\gamma^3 R^{(2)}\right\} \tag{38}$$

and

$$\frac{\beta\Delta P}{\bar{\rho}} = n_s\left\{-1 + \frac{1}{2}(\tau+1)\gamma - \frac{1}{2}n_s^2\bar{\rho}^2\gamma^2\left[L^2_\tau\left(\frac{\partial E^{(1,1)}}{\partial\bar{\rho}} + n_s\bar{\rho}\gamma\frac{\partial E^{(2,1)}}{\partial\bar{\rho}}\right) - \frac{1}{3}n_s\gamma\left(R^{(2)} - \bar{\rho}\frac{\partial R^{(2)}}{\partial\bar{\rho}}\right)\right]\right\}, \tag{39}$$

where $L_\tau = L + (1-L)\tau$,

$$\tau = \frac{1 + n_s\bar{\rho}\gamma LE}{1 + n_s\bar{\rho}\gamma(L-1)E} \tag{40}$$

and $E = E^{(1,1)} + n_s\bar{\rho}\gamma E^{(2,1)}$.

The corresponding expressions for the chemical potential $\Delta\mu$ in excess to its hard-sphere value and for the internal energy U follows from the standard relations:

$$\beta\Delta\mu = \frac{\beta\Delta P}{\bar{\rho}} + \frac{\beta\Delta A}{N} = n_s\ln\gamma - \frac{1}{2}n_s^2\bar{\rho}^2\gamma^2\left[L^2_\tau\left(\frac{\partial E^{(1,1)}}{\partial\bar{\rho}} + n_s\bar{\rho}\gamma\frac{\partial E^{(2,1)}}{\partial\bar{\rho}}\right) + \frac{1}{3}n_s\bar{\rho}\gamma\frac{\partial R^{(2)}}{\partial\bar{\rho}}\right] \tag{41}$$

and

$$\frac{\beta U}{N} = \beta\frac{\partial(\beta\Delta A)}{\partial\beta} = \frac{1}{2}n_s\beta\left[\left(\frac{2}{\gamma} - 1 - \tau - n_s^2\bar{\rho}^2\gamma^2 R^{(2)}\right)\frac{\partial\gamma}{\partial\beta} - \gamma\left(\frac{\partial\tau}{\partial\beta} + \frac{1}{3}n_s^2\bar{\rho}^2\gamma^2\frac{\partial R^{(2)}}{\partial\beta}\right)\right], \tag{42}$$

where

$$\frac{\partial\gamma}{\partial\beta} = -\sum_{i=0}^{7}\frac{\partial a_i}{\partial\beta}\gamma^i \Bigg/ \sum_{i=1}^{7} i a_i\gamma^{i-1}. \tag{43}$$

Integrals $E^{(1,1)}$ and $E^{(2,1)}$, which enter expressions for thermodynamics of the system, as well as their density and temperature derivatives are calculated following the scheme developed in Ref. 7. We briefly outlined the scheme and present the final expressions in the Appendix B. Fraction of the particles $X_{i_Ai_B\ldots}$ in a certain bonding state represented by the set $i_Ai_B\ldots$ can be also expressed in terms of γ-parameter. Combining Eqs. (7) and (12) we have

$$X_{i_Ai_B\ldots} = \frac{\bar{\rho}_{i_Ai_B\ldots}}{\bar{\rho}} = X_{\{0\}}(\tau-1)^{\sum_K i_K(2-i_K)}(\gamma^{-1}-\tau)^{\frac{1}{2}\sum_K i_K(i_K-1)} \tag{44}$$

where $X_{\{0\}} = \gamma^{n_s}$.

Finally, we note that all expressions for the thermodynamical properties derived above reduce to the corresponding expressions obtained in our previous study[1,2] upon neglecting contribution from three-particle correlations, i.e., assuming that $E^{(2,1)} = R^{(2)} \equiv 0$.

IV. RESULTS AND DISCUSSION

In this section we present and discuss numerical results for the two-patch version of the model. The model is represented by a fluid of hard spheres with two equivalent patchy sites A and B, symmetrically placed on the opposite sides of each sphere. The strength of interaction between patches is the same for each pair, i.e., $\epsilon_{AA} = \epsilon_{AB} = \epsilon_{BB} = \epsilon$. The width of the square-well site-site potential was chosen to be $r^{(c)} = 1.1d$ and the models are studied at different values of the limiting angle $\theta^{(c)}$. For the model at hand the coefficient L, which is defined by Eq. (23), will take the following form: $L = E^{(2,2)}/(E^{(1,1)})^2$. This coefficient was calculated and parameterized in Ref. 1. Solution of the polynomial equation (37) for the key parameter of the theory γ was obtained numerically using Newton-Raphson method. For the initial guess we have used the value of γ at infinitely large temperature, i.e., $\beta \to 0$. In this limit all the coefficients of the polynomial in (37), except a_0 and a_1, are equal zero and for the only one root we have $\gamma = 1$. Usually, we start at relatively high temperature and gradually lower it until the state point of interest is reached. To be sure that our solution is physical and in the limit of infinitely large temperature it has a correct asymptotic value we monitor the smoothness of variation of the solution variable γ while changing the temperature.

To validate the accuracy of the present theory we compare its predictions for thermodynamic properties and for the fractions of the patches in different bonding states $X_i^{(p)}$ $(i = 0, 1, 2)$ against corresponding computer simulation predictions and predictions of the RTPT-CF[2] at different values of the density $\bar{\rho}$, limiting angle $\theta^{(c)}$, and depth of the square-well site-site potential $\epsilon^* = \epsilon/k_BT$. Here $X_i^{(p)} = X_{i_A}^{(p)} + X_{i_B}^{(p)}$, where $i_A = i_B = i$, $X_{i_K}^{(p)}$ denote fraction of i_K-times bonded K-patches. $X_i^{(p)}$ is related to the fraction of the particles $X_{i_A j_B} \equiv X_{ij}$ in the bonding state $i, j \equiv i_A, j_B$ by the following relation

$$X_i^{(p)} = \sum_{j=0}^{2} X_{ij}, \tag{45}$$

where equivalence of the patches have been used, i.e., $X_{ij} \equiv X_{ji}$. Note that the density of the patches in the system is $\rho^{(p)} = 2\bar{\rho}$.

In order to obtain exact values for the multiply bondable patch model, we have performed a series of Monte Carlo (MC) simulations. Specifically, we determined the internal energy and fractions of the particles in different bonding states at different values of the system density from NVT (constant number of particles N, volume V, and temperature T) simulations while the density of the system as a function of pressure was calculated using NPT (constant N, T, and pressure P) simulations. For each simulation we used N = 864 colloids. Each NVT simulation was allowed to equilibrate for $N \times 10^6$ trial moves and averages were taken over an additional $N \times 10^6$ trial moves for association energies $\epsilon^* = \epsilon_{AB}/k_BT \leq 8$. A trial move consists of an attempted displacement and reorientation of a colloid. For the highest energy simulations $\epsilon^* = 8.5$ averages were taken over $4N \times 10^6$ trial moves. NPT simulations were performed in the same manner as NVT with the addition of an attempted volume change each N trial moves.

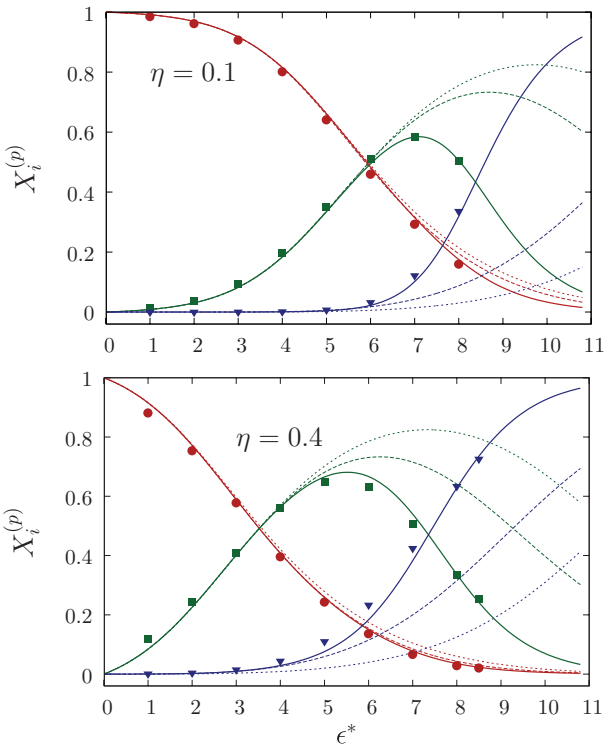

FIG. 1. Fractions of the patches in different bonding states $X_i^{(p)}$ as a function of the site-site square-well potential depth $\epsilon^* = \epsilon/k_BT$ at $\eta = 0.1$ (upper panel) and $\eta = 0.4$ (lower panel). Symbols denote computer simulation results, solid lines denote results of the current RTPT2-CF theory, dashed and dotted lines denote results of the RTPT-CF theory[1,2] with and without empirical correction for the ring formation, respectively. Here $X_0^{(p)}$ is represented by circles, $X_1^{(p)}$ by squares and $X_2^{(p)}$ by triangles.

Our theoretical and computer simulation results are shown in Figures 1–5. In Figures 1–4 we compare predictions of the current RTPT2-CF theory and RTPT-CF theory with and without empirical correction for the ring formation developed previously[2] against exact computer simulation predictions.

In Figure 1 we present fractions of the patches in different bonding states $X_i^{(p)}$ as a function of the site-site square-well potential depth $\epsilon^* = \epsilon/k_BT$ at two different values of the system packing fraction, i.e., $\eta = \pi\bar{\rho}d^3/6 = 0.1$ and $\eta = 0.4$. As one would expect, the fraction of free (non-bonded) patches $X_0^{(p)}$ decreases with increasing square-well depth ϵ^*. At the same time, the fraction of doubly bonded patches $X_2^{(p)}$ remains small up to the value of the square-well depth $\epsilon^* = 6$ at $\eta = 0.1$ and $\epsilon^* = 4$ for $\eta = 0.4$. In this range the fraction of singly bonded patches $X_1^{(p)}$ increases. However, with further increase of ϵ^* $X_2^{(p)}$ starts to grow rapidly and $X_1^{(p)}$, after reaching the maximum value at $\epsilon^* \approx 7$ $(\eta = 0.1)$ and $\epsilon^* \approx 5.4$ $(\eta = 0.4)$, decreases. This behaviour

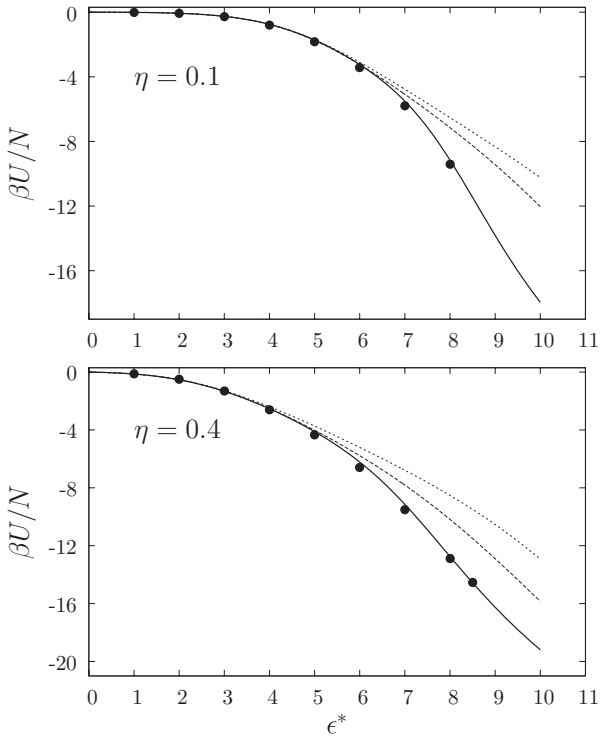

FIG. 2. Internal energy $\beta U/N$ per particle as a function of the site-site square-well potential depth $\epsilon^* = \epsilon/k_BT$ at $\eta = 0.1$ (upper panel) and $\eta = 0.4$ (lower panel). Symbols denote computer simulation results, solid lines denote results of the current RTPT2-CF theory, dashed and dotted lines denote results of the RTPT-CF theory[1,2] with and without empirical correction for the ring formation, respectively.

of $X_1^{(p)}$ and $X_2^{(p)}$ reflects the competition between formation of small size clusters of particles at low values of ϵ^* and large size clusters of particles at larger values of ϵ^*. Predictions of the current theory are in excellent agreement with computer simulation predictions. Predictions of RTPT-CF approach developed in Ref. 2 are accurate only at low and intermediate values of ϵ^*, up to $\epsilon^* \approx 6$ for $\eta = 0.1$ and $\epsilon^* \approx 4.5$ for $\eta = 0.4$. For larger ϵ^* both versions of the theory give substantially less accurate results, with empirically corrected version being slightly more accurate.

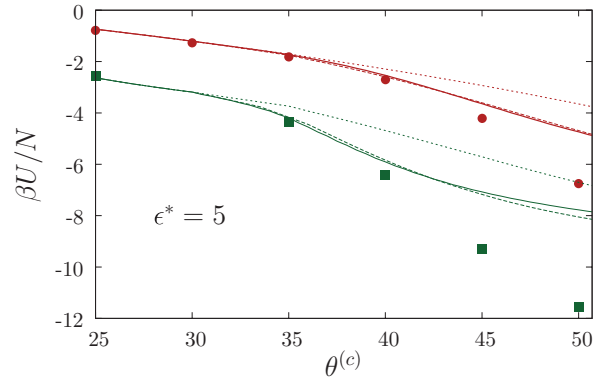

FIG. 3. Internal energy $\beta U/N$ per particle as a function of the critical angle $\theta^{(c)}$. Symbols denote computer simulation results, solid lines denote results of the current RTPT2-CF theory, dashed and dotted lines denote results of the RTPT-CF theory[1,2] with and without empirical correction for the ring formation, respectively. Here $\epsilon^* = 5$ and $\eta = 0.1$ (circles and upper set of the curves) and $\eta = 0.4$ (squares and lower set of the curves).

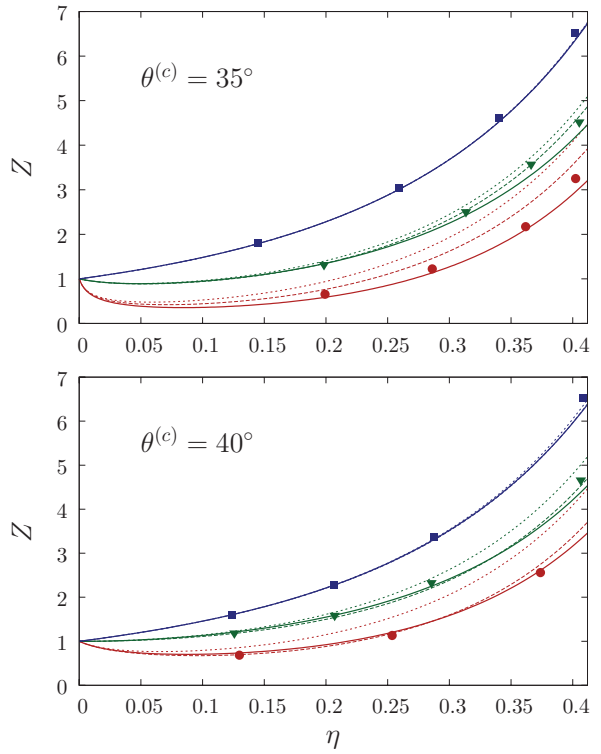

FIG. 4. Compressibility factor $Z = \beta PV/N$ as a function of the packing fraction $\eta = \pi\rho d^3/6$ for the models with $\theta^{(c)} = 35°$ (upper panel) and $\theta^{(c)} = 40°$ (lower panel) at different values of the site-site square-well potential depth $\epsilon^* = \epsilon/k_BT$. Symbols denote computer simulation results, solid lines denote results of the current RTPT2-CF theory, dashed and dotted lines denote results of the RTPT-CF theory[1,2] with and without empirical correction for the ring formation, respectively. Here on the upper panel squares denote results for $\epsilon^* = 2$, triangles for $\epsilon = 5.556$ and circles for $\epsilon^* = 7.692$. On the lower panel squares stand for $\epsilon^* = 2$, triangles for $\epsilon^* = 4.17$, and circles for $\epsilon^* = 5.556$.

Our predictions for the internal energy per particle $\beta U/N$ are shown in Figure 2. Results of the current theory are in very good agreement with MC results. Similar to the previous results RTPT-CF theory appears to be accurate at low and intermediate values of ϵ^*. In Figure 3 we present internal energy

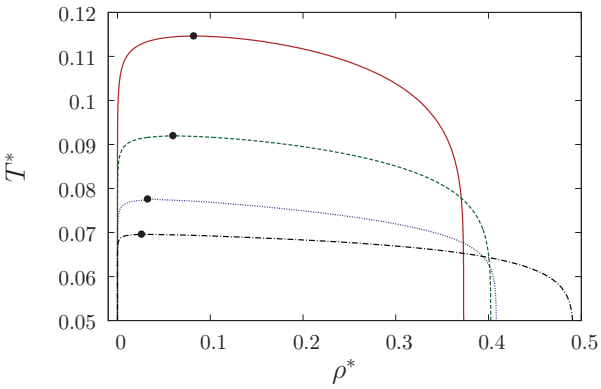

FIG. 5. Liquid-gas phase diagram of the model with $\theta^{(c)} = 35°$ (solid line), $\theta^{(c)} = 32°$ (dashed line), $\theta^{(c)} = 31°$ (dotted line), and $\theta^{(c)} = 30.1°$ (dashed-dotted line). Circles denote the critical points, $\rho^* = \bar{\rho}d^3$ and $T^* = 1/\epsilon^*$.

as a function of the critical angle $\theta^{(c)}$ at $\epsilon^* = 5$ and two values of the packing fraction, $\eta = 0.1$ and $\eta = 0.4$. We note in passing that for $\theta^{(c)} > 35.3^\circ$ more than two bonds per patch can be formed. However, the present theory is formulated for doubly bondable patches, it can be applied also for $\theta^{(c)} > 35.3^\circ$. According to Figure 3 agreement between theory and simulation at a moderate value of $\epsilon^* = 5$ is reasonable up to $\theta^{(c)} = 40^\circ$. Comparison of the theoretical and computer simulation predictions for the compressibility factor $Z = \beta P/\bar{\rho}$ as a function of the packing fraction η at different values of ϵ^* and two values of the critical angle $\theta^{(c)} = 35^\circ$ and $\theta^{(c)} = 40^\circ$ are shown in Figure 4. The overall agreement between current theory and computer simulation is very good, including the region of higher values of ϵ^*. For these values of ϵ^*, the behaviour of the system is defined by the formation of the three-patch rings, which is accurately accounted for by the theory. For intermediate values of ϵ^* and higher values of η, where formation of the chains of patches is prevailing, our theory is slightly less accurate. Predictions of the two versions of RTPR-CF theory are less accurate, especially at higher ϵ^*. Here RTPT-CF approach corrected for the ring formation is slightly more accurate, in particular for $\theta^{(c)} = 40^\circ$ and lower ϵ^*. Good agreement for this particular case can be attributed to a fortuitous cancellation of the errors.

Finally, in Figure 5 we present liquid-gas phase diagrams of the model with different values of the critical angle $\theta^{(c)}$, i.e., $\theta^{(c)} = 35^\circ, 32^\circ\, 31^\circ, 30.1^\circ$. For the limiting case of $\theta^{(c)} = 30^\circ$ (and sufficiently narrow square-well potential) the particles of the system will form only chains and there will be no liquid-gas phase coexistence. This tendency is correctly predicted by the current theory, i.e., upon decreasing of $\theta^{(c)}$ the critical temperature and density decrease, moving towards their zero values.

V. CONCLUSIONS

In this paper we propose a second-order resummed thermodynamic perturbation theory for the patchy colloidal model with an arbitrary number of doubly bondable patches. Second-order terms are included to account for the formation of rings and chains of the patches. The theory explicitly takes into account blocking effects, i.e., when bonding of the particle blocks bonding on the same associating site by other particles. In the limiting case of total blockage, when creation of only one bond per site is possible, our RTPT-CF approach reduces to Wertheim TPT for polymerization.[37] We obtain closed-form analytical expressions for thermodynamical properties (Helmholtz free energy, pressure, chemical potential, and internal energy) of the model with n_s equivalent patches. To validate the accuracy of the present theory we compare its predictions for the fractions of the patches in different bonding states and for thermodynamical properties of the two-patch version of the model against new Monte Carlo computer simulation predictions and predictions of the first-order RTPT-CF[2] at different values of the density, limiting angle and depth of the square-well potential. Results of the current theory are found to be in very good agreement with computer simulation results, including the region of strong association, where the first-order RTPT-CF appears to be substantially less accurate. The accuracy of the theoretical predictions for the models with larger number of the patches will be studied in subsequent papers. For future work we are planning to apply the version of our theory developed for the model with two patches to describe the phase behaviour of triblock Janus colloids.[39–41]

ACKNOWLEDGMENTS

We would like to thank Ukrainian Academic Grid for computing resources.

APPENDIX A: EXPRESSIONS FOR THE COEFFICIENTS OF THE POLYNOMIAL EQUATION (37)

Expressions for the coefficients a_i of the polynomial equation (37) are

$$a_0 = -1, \qquad a_1 = 1 - 2\rho_n L_1 E_1,$$

$$a_2 = -\rho_n \left[2\left(\rho_n E_2 - E_1\right) L_1 + \left(\rho_n L_1^2 E_1 - 1\right) E_1\right],$$

$$a_3 = -\frac{1}{2}\rho_n^2 \big[2(2\rho_n E_2 - E_1) L_1^2 E_1 - \left(4E_2 + E_1^2\right) L_1 - 3E_2 - R_2\big],$$

$$a_4 = -\rho_n^3 L_1 \left[\left(\rho_n E_2 - 2E_1\right) E_2 L_1 - \left(E_2 + R_2\right) E_1\right],$$

$$a_5 = \frac{1}{2}\rho_n^4 L_1 \left[\left(2E_2^2 + R_2 E_1^2\right) L_1 + \left(E_2 + 2R_2\right) E_2\right],$$

$$a_6 = \rho_n^5 L_1^2 R_2 E_1 E_2, \qquad a_7 = \frac{1}{2}\rho_n^6 L_1^2 R_2 E_2^2,$$

where $\rho_n = n_s \bar{\rho}$, $L_1 = L - 1$, $E_1 = E^{(1,1)}$, $E_2 = E^{(2,1)}$ and $R_2 = R^{(2)}$.

APPENDIX B: EXPRESSIONS FOR THE INTEGRALS $E^{(1,1)}$, $E^{(2,1)}$, AND $R^{(2)}$

For the model at hand expressions for the integrals $E^{(1,1)}$, $E^{(2,1)}$ (21), and $R^{(2)}$ (17) are

$$E^{(1,1)} = \Omega^{-1} \int d(2) f_{ass}(12) g_{hs}(r_{12}), \tag{B1}$$

$$E^{(2,1)} = \Omega^{-2} \int d(2) d(3) f_{ass}(12) f_{ass}(23) [g_{hs}(r_{12}, r_{23}, r_{32}) - g_{hs}(r_{12}) g_{hs}(r_{23}) e_{hs}(r_{13})], \tag{B2}$$

and

$$R^{(2)} = \Omega^{-2} \int d(2) d(3) f_{ass}(12) f_{ass}(23) f_{ass}(31) g_{hs} \times (r_{12}, r_{23}, r_{13}) \tag{B3}$$

where $f_{ass}(ij) \equiv f_{KL}(ij)$, $e_{hs}(r_{ij}) = f_{hs}(r_{ij})$, and $r_{ij} = |\vec{r}_i - \vec{r}_j|$.

TABLE I. Geometric integrals Γ and Ψ and averaged constants $\bar{a}_j$ and $\bar{b}_j$ as a function of $\theta^{(c)}$.

$\theta^{(c)}$	Γ	Ψ	$\bar{a}_{ch}$	$\bar{b}_{ch}$	$\bar{a}_{rng}$	$\bar{b}_{rng}$
30°	8.47×10^{-8}	0	−1.7568	1.5779		
31°	2.92×10^{-7}	1.81×10^{-12}	−1.7752	1.5281	−1.7780	1.5238
32°	7.35×10^{-7}	1.29×10^{-10}	−1.8004	1.4883	−1.8126	1.4698
33°	1.54×10^{-6}	1.19×10^{-9}	−1.8254	1.4539	−1.8410	1.4327
34°	2.85×10^{-6}	5.22×10^{-9}	−1.8505	1.4243	−1.8681	1.4015
35°	4.88×10^{-6}	1.60×10^{-8}	−1.8755	1.3992	−1.8795	1.3896
40°	3.62×10^{-5}	4.51×10^{-7}	−1.9976	1.3334	−1.8928	1.3750
45°	1.49×10^{-4}	3.18×10^{-6}	−2.1121	1.3427	−1.8947	1.3730
50°	4.56×10^{-4}	1.29×10^{-5}	−2.2155	1.3976	−1.8956	1.3720
55°	1.16×10^{-3}	3.87×10^{-5}	−2.3060	1.4748	−1.8957	1.3720

These integrals are calculated following closely the scheme developed in Ref. 7. Therefore, to avoid unnecessary repetition we refer the readers to the original paper for details and present here only the final expressions. We have

$$E^{(1,1)} = \pi d^2(e^{\beta\epsilon} - 1)(r^{(c)} - d)(1 - \cos\theta^{(c)})^2 g_{hs}(d^+), \tag{B4}$$

$$E^{(2,1)} = d^6(e^{\beta\epsilon} - 1)^2\left(y_{ch}^{(0)} - 1\right)g_{hs}^2(d^+)\Gamma, \tag{B5}$$

and

$$R^{(2)} = d^6(e^{\beta\epsilon} - 1)^3 y_{rng}^{(0)}\ g_{hs}^2(d^+)\Psi. \tag{B6}$$

The correlation functions $y_{ch}^{(0)}$ and $y_{rng}^{(0)}$ represent the correction to a linear superposition of the hard sphere reference triplet correlation function, for three spheres in rolling contact, for a triplet chain and triplet ring, respectively. Mueller and Gubbins[38] correlated this quantity as a function of bond angle ω as $y^{(0)} = (1 + a\eta + b\eta^2)/(1 - \eta)^3$ where a and b are constants which depend on ω and are tabulated in the original paper.[38] For our case $\theta^{(c)}$ is fixed not ω. In our previous work we used an average $\bar{\omega}_j$ ($j = ch, rng$) which represents the average bond angle in the respective triplet cluster when all bonds are at hard sphere contact to obtain an average $\bar{a}_j$ and $\bar{b}_j$ to evaluate $y_j^{(0)}$ as

$$y_j^{(0)} = \frac{1 + \bar{a}_j\eta + \bar{b}_j\eta^2}{(1 - \eta)^3}. \tag{B7}$$

In this work we take a more accurate approach and obtain $\bar{a}_j$ and $\bar{b}_j$ by averaging a and b over the states of the respective associated cluster, when the first and third sphere in the cluster are bonded at hard sphere contact to the second, using the MC technique. Table I gives these averaged constants as well as the geometric integrals Γ and Ψ which are proportional to the total number of ways three colloids can associate into a chain and ring, respectively. Γ and Ψ are discussed in detail in Ref. 7 and are evaluated using MC integration. To obtain good statistics in evaluating Ψ for smaller $\theta^{(c)}$ a more sophisticated nested coordinate system was used in comparison to Ref. 7. For this reason there is a very slight change to Ψ at $\theta^{(c)} = 35°$, 40° from the previously reported values.

[1] Y. V. Kalyuzhnyi, H. Docherty, and P. T. Cummings, J. Chem. Phys. **133**, 044502 (2010).
[2] Y. V. Kalyuzhnyi, H. Docherty, and P. T. Cummings, J. Chem. Phys. **135**, 014501 (2011).
[3] Y. V. Kalyuzhnyi and G. Stell, Mol. Phys. **78**, 1247 (1993).
[4] Y. V. Kalyuzhnyi, I. A. Protsykevitch, and P. T. Cummings, Europhys. Lett. **80**, 56002 (2007).
[5] Y. V. Kalyuzhnyi, I. A. Protsykevitch, and P. T. Cummings, Condens. Matter Phys. **10**, 553 (2007).
[6] M. S. Wertheim, J. Stat. Phys. **35**, 19–34 (1984).
[7] B. D. Marshall, D. Ballal, and W. G. Chapman, J. Chem. Phys. **137**, 129902 (2012).
[8] B. D. Marshall and W. G. Chapman, J. Chem. Phys. **138**, 044901 (2013).
[9] R. P. Sear and G. Jackson, Phys. Rev. E **50**, 386 (1994).
[10] V. N. Manoharan, M. T. Elsesser, and D. J. Pine, Science **301**, 483 (2003).
[11] A. van Blaaderen, Nature (London) **439**, 545 (2006).
[12] S. C. Glotzer and M. J. Solomon, Nature Mater. **6**, 557 (2007).
[13] W. Bol, Mol. Phys. **45**, 605 (1982).
[14] W. R. Smith and I. Nezbeda, J. Chem. Phys. **81**, 3694 (1984).
[15] J. Kolafa and I. Nezbeda, Mol. Phys. **61**, 161 (1987).
[16] J. Kolafa and I. Nezbeda, Mol. Phys. **72**, 777 (1991).
[17] G. Jackson, W. G. Chapman, and K. E. Gubbins, Mol. Phys. **65**, 1 (1988).
[18] N. Kern and D. Frenkel, J. Chem. Phys. **118**, 9882 (2003).
[19] M. S. Wertheim, J. Chem. Phys. **85**, 2929 (1986).
[20] I. Nezbeda, J. Kolafa, and Y. V. Kalyuzhnyi, Mol. Phys. **68**, 143 (1989).
[21] M. F. Holovko and Y. V. Kalyuzhnyi, Mol. Phys. **73**, 1145 (1991).
[22] Y. V. Kalyuzhnyi, M. F. Holovko, and I. A. Protsykevytch, Chem. Phys. Lett. **215**, 1 (1993).
[23] M. Holovko and J. P. Badiali, Chem. Phys. Lett. **204**, 511 (1993).
[24] Y. V. Kalyuzhnyi, G. Stell, M. L. Llano-Restrepo, W. G. Chapman, and M. F. Holovko, J. Chem. Phys. **101**, 7939 (1994).
[25] J. E. Chang and S. I. Sandler, J. Chem. Phys. **102**, 437 (1995).
[26] Y. V. Kalyuzhnyi, C.-T. Lin, and G. Stell, J. Chem. Phys. **106**, 1940 (1997).
[27] E. Vakarin, Y. Duda, and M. F. Holovko, Mol. Phys. **90**, 611 (1997).
[28] C.-T. Lin, Y. V. Kalyuzhnyi, and G. Stell, J. Chem. Phys. **108**, 6513 (1998).
[29] Y. V. Kalyuzhnyi and V. Vlachy, J. Chem. Phys. **108**, 7870 (1998).
[30] Y. V. Kalyuzhnyi and M. F. Holovko, J. Chem. Phys. **108**, 3709 (1998).
[31] Y. V. Kalyuzhnyi, L. Blum, J. Rescic, and G. Stell, J. Chem. Phys. **113**, 1135 (2000).
[32] Y. V. Kalyuzhnyi and P. T. Cummings, J. Chem. Phys. **118**, 6437 (2003).
[33] Y. V. Kalyuzhnyi, C. R. Iacovella, H. Docherty, M. Holovko, and P. T. Cummings, J. Stat. Phys. **145**, 481 (2011).
[34] F. Sciortino, Collect. Czech. Chem. Commun. **75**, 349 (2010).
[35] E. Bianchi, R. Blaak, and C. N. Likos, Phys. Chem. Chem. Phys. **13**, 6397 (2011).
[36] M. S. Wertheim, J. Stat. Phys. **42**, 477–495 (1986).
[37] M. S. Wertheim, J. Chem. Phys. **87**, 7323 (1987).
[38] E. Muller and K. Gubbins, Mol. Phys. **80**, 957 (1993).
[39] Q. Chen, S. C. Bae, and S. Granick, Nature (London) **469**, 381 (2011).
[40] A. Giacometti, F. Lado, J. Largo, G. Pastore, and F. Sciortino, J. Chem. Phys. **132**, 174110 (2010).
[41] F. Romano and F. Sciortino, Soft Matter **7**, 5799 (2011).